Conceptual Models of Precipitation Systems*,@

KEITH A. BROWNING

Meteorological Office, Bracknell, Berkshire RG12 2SZ, United Kingdom

(Manuscript received and in final form 10 December 1985)

ABSTRACT

Imagery from radars and satellites is one of the main ingredients of nowcasting. When used to provide very detailed forecasts of precipitation for a few hours ahead, the imagery needs to be interpreted carefully in terms of synoptic and mesoscale phenomena and their mechanisms. This paper gives an overview of some conceptual models that are useful for this purpose. The models represent a variety of systems associated with midlatitude cyclones and also mesoscale convective systems in the tropics and midlatitudes. Specific phenomena discussed are

- warm conveyor belts, including those with rearward- and forward-sloping ascent in ana and kata cold frontal situations, respectively;
- cold conveyor belts ahead of warm fronts;
- narrow rainbands associated with line convection at the boundary of a pre-cold-frontal low-level jet;
- wide mesoscale rainbands associated with midtropospheric convection;
- squall lines in the tropics and midlatitudes;
- nonsquall mesoscale convective systems in the tropics and midlatitudes;
- subsynoptic-scale comma clouds associated with cold-air vortices;
- polar-trough conveyor belts and instant occlusions.

1. Introduction

Nowcasting, i.e., the generation of detailed site-specific forecasts for a few hours ahead, is a particularly challenging task in the presence of precipitation-producing weather systems. This is partly because of the difficulty in observing these systems adequately, owing to the large amount of mesoscale and convective substructure they contain. It is also because of the difficulty in predicting how these complex patterns will evolve even in the very short term.

Direct in situ measurements by themselves do not offer an adequate means of observing on the mesoscale. Satellite-based measurements and ground-based radar observations, on the other hand, do provide a good opportunity for describing many of the fine-scale features, especially the cloud and precipitation patterns. Mesoscale temperature information is not so easily obtained, because, for example, of the problem of retrieving satellite soundings when the field of view is contaminated by cloud and precipitation. It is, however, possible to make useful inferences about the fields of airflow (and to a limited extent the location of temperature gradients) from the form and movement of these same cloud and precipitation patterns, although this calls for some subjective interpretation of the patterns.

Subjective interpretation is even more necessary in the generation of very short-range forecasts. It is well known that simple objective extrapolation alone is of only limited value for forecasting precipitation and that, in order to obtain an indication of probable areas of development and decay, it is necessary to be able to infer where the areas of potential instability and slantwise ascent are likely to be. Numerical models can provide guidance about the broader scale features, but even if mesoscale models are used subjective interpretation is often still needed to unravel the complexity of the mesoscale.

Until recently, a major factor impairing the forecaster's ability to exploit satellite- and radar-imagery has been the inadequacy of the systems for displaying and manipulating the data. Forecasters are, however, beginning to be provided with modern display systems, sometimes with facilities for action replay, image reprojection and enhancement, and, in a few cases, superimposed model products. The primary impediment to using these data effectively is now the forecaster's limited ability to make sense of the cloud and precipitation patterns in terms of the dynamical factors that are producing them. There is thus a clear need for more training of forecasters in the meteorological interpretation of the imagery. As part of this training, the forecaster needs to be provided with a better conceptual framework within which to interpret the imagery. In

@ Previously published in *Meteor. Mag.*, **114**, 293–319, and ESA Journal, 1985, Vol. 9, 157–180.

short, he needs a set of conceptual models of precipitation systems. These same conceptual models can be expected to be helpful in interpreting not only the imagery, but also numerical model guidance in terms of surface weather, especially where the forecaster is able to display sequences of satellite- and radar-imagery superimposed on the model predictions for corresponding times.

The purpose of this paper is to present some examples of conceptual models that are thought to be helpful in the interpretation of imagery. The paper's scope is limited to mesoscale precipitation systems and their larger scale context. Both frontal systems and convective systems are discussed. The emphasis is mainly, but not entirely, on midlatitude systems. Individual thunderstorms are not considered. Terrain effects, though important, are also excluded.

2. Conveyor-belt models applicable to midlatitude frontal systems

The frontal models of the Norwegian school have dominated our ideas of frontal structure for over half a century. Forecasters still struggle to interpret mesoscale details of midlatitude precipitation systems within the context of the simple archetypes of the warm, cold and occluded front. These models are at best inadequate and at worst misleading, and an overdependence on them has tended to bring frontal analysis into disrepute. However, the task of improving on the existing models is not an easy one. In this paper, therefore, we can present only a few faltering steps towards a new conceptual approach in frontal analysis.

The first requirement for analyzing the mesoscale features of cloud and precipitation in frontal systems is to have a synoptic-scale framework that is able to reconcile the observations in a natural (i.e., system-centered) way. A concept that has been found useful is based on the idea of the conveyor belt, the essence of which is that it identifies the major cloud and precipitation-producing flows in a *system-relative frame of reference.*

a. The warm conveyor belt

The dominant mechanism in frontal systems is baroclinic slantwise ascent, and Fig. 1, from Green et al. (1966), shows a simplified depiction of the corresponding large-scale pattern of flow in a major trough–ridge system. The key feature is the elongated band of cloud that forms along the boundary of a major confluence zone at the leading edge of the trough. In a frame of reference moving with the trough–ridge system, warm air is seen to be drawn into the cloud belt from the convective boundary layer at low latitudes; it rises into the middle troposphere as it travels within the cloud belt and eventually produces a deck of upper tropospheric cirrus which decays ahead of the frontal system. Following Harrold (1973), we refer to the narrow airstream as the warm conveyor belt, because of its role in conveying large quantities of heat (and also moisture and westerly momentum) poleward and upward. The region of cirrus cloud associated with it is referred to by Weldon (1979) as baroclinic-zone cirrus.

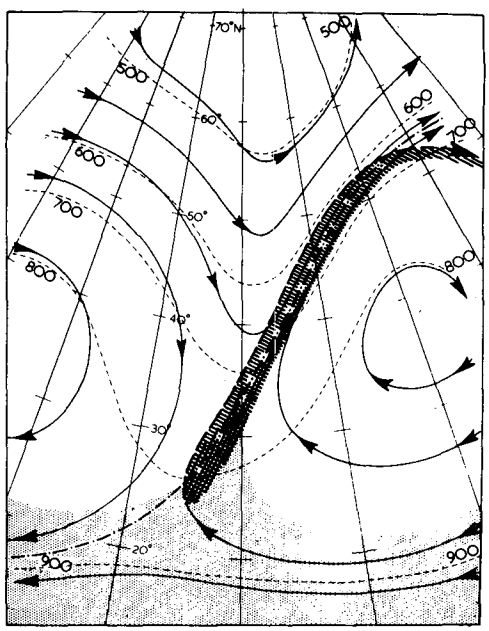

FIG. 1. Schematic representation of relative flow in a major trough of large-scale slantwise convection over an ocean, on a surface of constant potential temperature Θ (about 30°C). The height of the surface is shown by dashed lines (in mb). The cold frontal zone, in which the narrowing of the separation between two isobars indicates a steepening of the isentropic surface, contains a (dot-dashed) line of confluence between two principal airstreams. The stippled zone in the south shows where trajectories of the mean flow lie within the layer of small-scale convection in the boundary layer in which Θ, and even more so wet-bulb potential temperature Θ_w, increase along the flow. The air is unsaturated in most areas, except for the hatched area which marks a band of clouds rising above the isentropic surface. This is the region of strong south to southwesterly flow which we refer to as the warm conveyor belt. The clouds in the warm conveyor belt first form at low latitudes, where they are liable to develop into more or less deep convective clouds (in the region shown by cross-hatching); they appear subsequently as middle-level layer clouds, and eventually as ice clouds (baroclinic cirrus) in the high troposphere of middle latitudes (where they lie near and to the right of the axis of the upper tropospheric jet stream). These clouds evaporate after the flow at their level has turned to become northwesterly and the airstream begins to subside (from Green et al., 1966).

The warm conveyor belt has been found to be a useful concept for accounting for frontal systems not only in northwestern Europe, where the idea first evolved, but also in the United States (Carlson, 1980) and Australia (Ryan and Wilson, 1985). Cahir et al. (1985) have carried out a composite analysis of a large number of warm conveyor belts and show that in these high-speed flows of warm moist air, the relative wind jet stream is situated within and closely parallel to the typically sharp left-hand cloud edge. An example of a well-defined cloud belt associated with a long warm

conveyor belt is given in Fig. 2. Warm conveyor belts vary greatly in length and are certainly not always as long as in Figs. 1 and 2.

Air in the warm conveyor belt flows along the length of the cold front, part of it often being in the form of a low-level jet within the boundary layer just ahead of the surface cold front (Browning and Pardoe, 1973). The warmest air of all, having originated farthest south, is usually to be found immediately ahead of the surface cold front. The associated, negative horizontal temperature gradient ahead of the cold front in the warm conveyor belt accounts, through the thermal wind relationship, for the decrease in wind speed above the low-level jet.

Although the main component of motion within the warm conveyor belt is parallel to the cold front, the relatively small and mainly ageostrophic component perpendicular to the front has an important bearing on the frontal structure. It is useful to distinguish two contrasting situations:

(i) A "rearward-sloping ascent" configuration, in which the air in the warm conveyor belt has a component of motion rearward relative to the movement of the cold front and in which the slantwise ascent occurs in the vicinity of and above the cold frontal zone;

(ii) A "forward sloping ascent" configuration, in which the air in and above the warm conveyor belt has a component of motion forward relative to the movement of the cold front, with its main region of slantwise ascent occurring farther downwind in regions of warm frontal baroclinicity.

Transitions between rearward- and forward-sloping ascent can occur both in time and in space (along the length of a cold front).

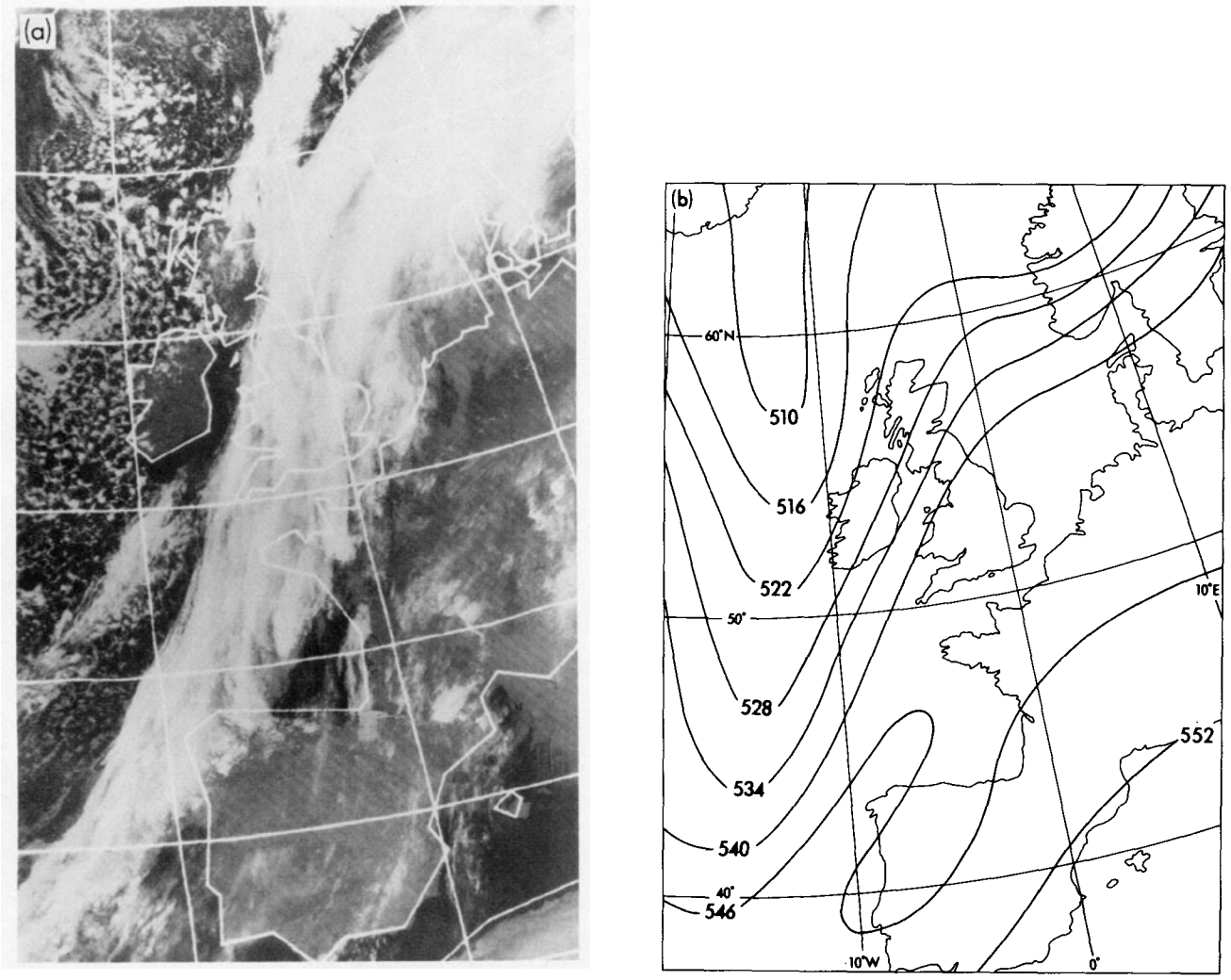

FIG. 2. (a) Infrared photograph from a NOAA satellite at 0317 GMT on 13 January 1983 showing an elongated belt of cloud associated with a major warm conveyor belt (Courtesy University of Dundee). (b) 1000–500 mb thickness analysis for 0000 GMT showing the major trough–ridge system with which the warm conveyor belt was associated.

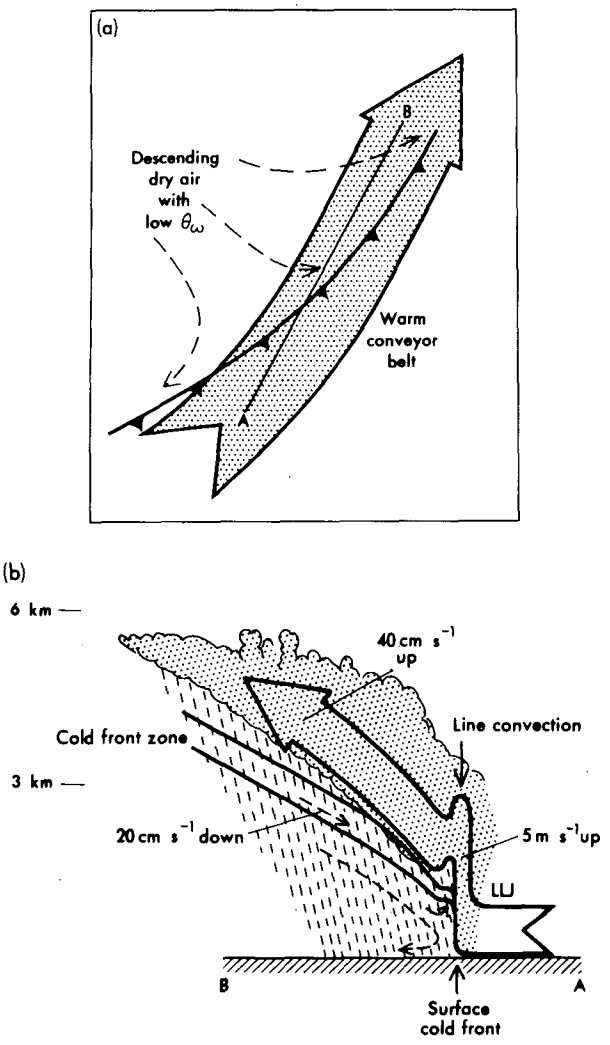

FIG. 3. Schematic portrayal of airflow at a classical ana cold front showing the warm conveyor belt (bold arrow) undergoing rearward-sloping ascent above the cold frontal zone with the cold air (dashed lines) descending beneath it: (a) plan view; (b) vertical section along *AB* in (a). Flows are shown relative to the moving frontal system. LLJ marks axis of low-level jet in (b).

b. The warm conveyor belt with rearward-sloping ascent

The rearward-sloping ascent configuration (Fig. 3), in which some or all of the warm conveyor-belt air rises with a component rearward above an advancing wedge of cold air, corresponds to the classical ana cold frontal situation (Sansom, 1951). In the United Kingdom, this configuration is not as common as the situation of forward-sloping ascent described in the next subsection. In contrast to situations of forward-sloping ascent, the surface cold front in cases of rearward-sloping ascent tends to be sharp. The warm air in the boundary layer ahead of the surface cold front is lifted abruptly at up to several meters per second within a narrow strip adjacent to the surface cold front. This is a region of intense cyclonic shear (10^{-2} s^{-1}) on the western boundary of the pre-cold-frontal low-level jet, and the vertical air velocity is consistent with the expected Ekman-layer convergence. Release of latent heat in the presence of friction has been shown to be an important factor contributing to the strength of both the low-level jet and the cyclonic shear (Hsie et al., 1984).

The air rises only 2 to 3 km during its abrupt ascent at the surface cold front. It undergoes further ascent in slantwise fashion, at a few tens of centimeters per second, above the wedge of cold air (Browning and Harrold, 1970). These two regions of ascent produce two distinct patterns of precipitation:

(i) a narrow band of very heavy rain at the surface cold front, and
(ii) a broad belt of light-to-moderate rain extending behind, and often to some extent ahead, of the surface cold front.

These features are discussed further later in the paper.

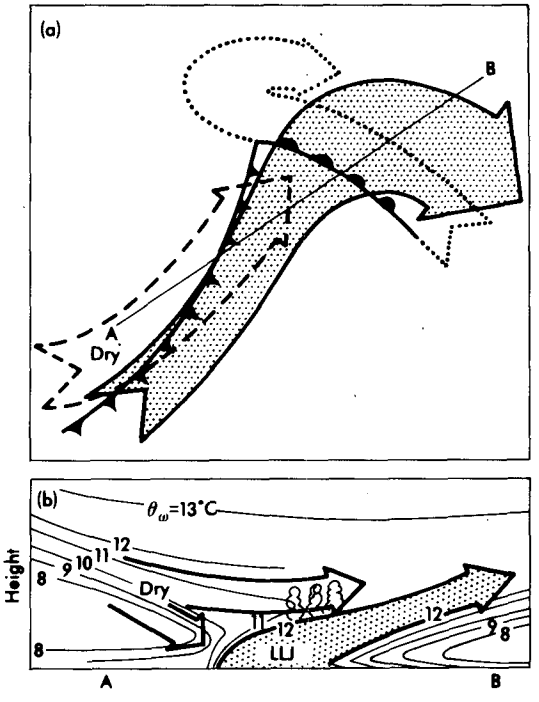

FIG. 4. Schematic portrayal of airflow in a midlatitude cyclone in which the warm conveyor belt (solid arrow with stippled shading) is undergoing forward-sloping ascent ahead of a kata cold front before rising above a flow of cold air ahead of the warm front (dotted arrow referred to later as the cold conveyor belt). Cold middle-tropospheric air with low Θ_w (dashed arrow) is shown overrunning the cold front and generating potential instability in the upper portions of the warm conveyor belt. Plan view and vertical section are shown in (a) and (b), respectively, the section in (b) being along the line *AB* in (a). Flows are shown relative to the moving frontal system.

c. The warm conveyor belt with forward-sloping ascent

The forward-sloping ascent configuration, shown in Fig. 4, corresponds to a kata cold-front situation for which the main ascent occurs ahead of the surface cold front and recently descended air with low wet-bulb potential temperature (Θ_w) overruns the warm conveyor belt in the middle troposphere (Miles, 1962). This leads to the generation of potential instability, which is realized as convection once the general flow has been lifted sufficiently. This convection sometimes occurs as deep convection from the surface, but more usually in the United Kingdom it occurs as shallow mid-level convection. Eventually, the cloudy, warm conveyor-belt flow turns anticyclonically (i.e., to the right) as it overtakes and ascends over the cold air ahead of the surface warm front. The convex poleward boundary to this flow, where it ascends and turns to the right, is often clearly detectable in satellite visible imagery from the shadow the upper cloud casts on the lower cloud layer.

The leading edge of the overrunning dry low-Θ_w air advancing ahead of the surface cold front often appears as a well-defined upper cold front (*UU* in Fig. 5a). Ahead of the upper cold front, the depth of the warm moist air increases abruptly in association with an organized band of convection. This gives a wide band of moderate-to-heavy rain, often at the trailing edge of a region of rather lighter warm frontal precipitation, much of which may evaporate before reaching the ground. The passage of the upper cold front is followed by a shallow moist zone (Fig. 5b) with scattered out-

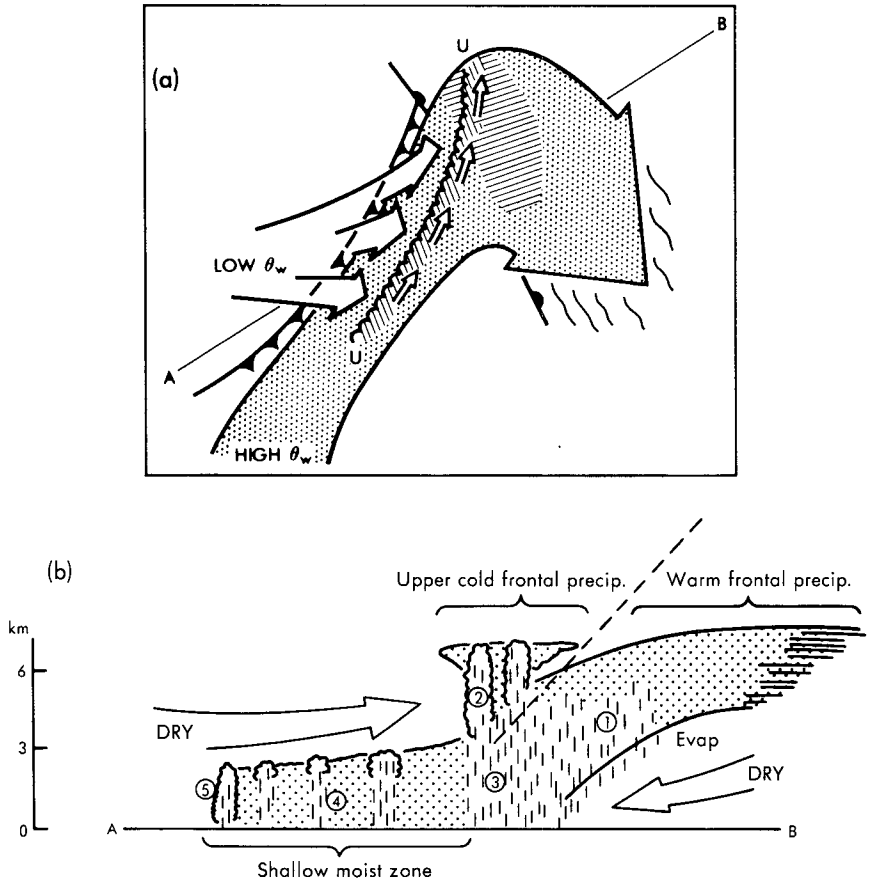

FIG. 5. Schematic portrayal of the same situation as in Fig. 4, i.e., with the warm conveyor belt undergoing forward-sloping ascent but drawing attention to the split-front characteristic and the overall precipitation distribution: (a) plan view; (b) vertical section along *AB* in (a). In (a) *UU* represents the upper cold front. The hatched shading along *UU* and ahead of the warm front represents precipitation associated with the upper cold front and warm front, respectively. Numbers in (b) represent precipitation type as follows: 1) warm frontal precipitation, 2) convective precipitation-generating cells associated with the upper cold front, 3) precipitation from the upper cold frontal convection descending through an area of warm advection, 4) shallow moist zone between the upper and surface cold fronts characterized by warm advection and scattered outbreaks of mainly light rain and drizzle, and 5) shallow precipitation at the surface cold front itself (after Browning and Monk, 1982).

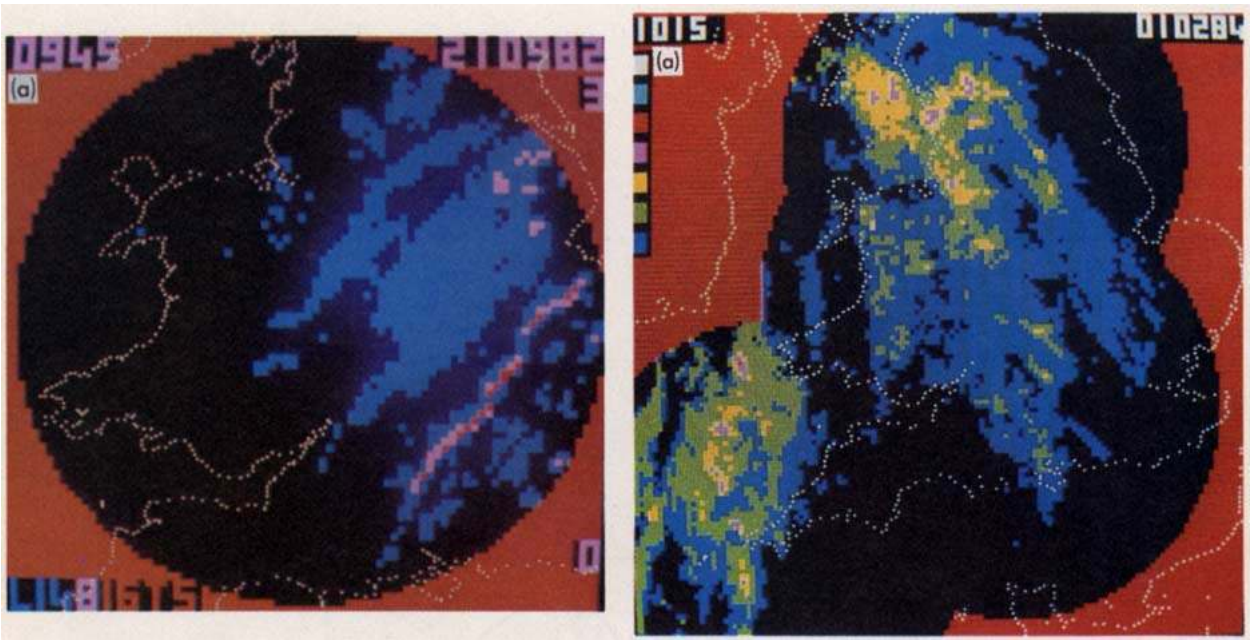

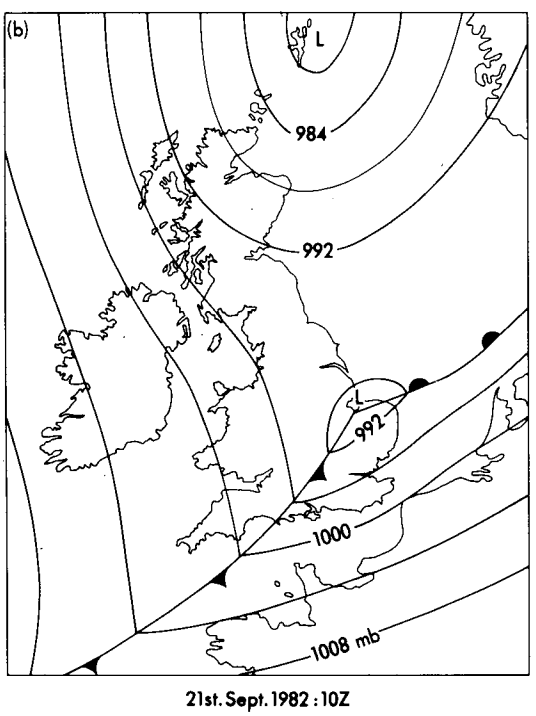

FIG. 6. (a) Plan radar display showing a narrow cold frontal rainband over England. Pink and red, heavy rain mostly associated with the narrow rainband; blue, light and moderate rain. Resolution is 5 km × 5 km. (b) Surface analysis corresponding to (a).

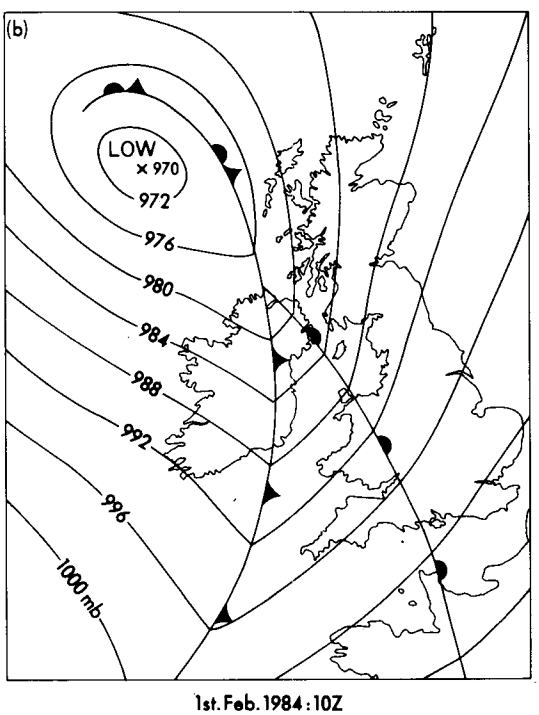

FIG. 7. (a) Plan radar network display showing wide frontal rainbands. Those over northern and central England are associated with a warm front. Those in the southwestern approaches are associated with a cold front. The ill-defined, ragged nature of these bands is typical of wide rainbands. Some of the complexity (not all) is due to orographic effects. Pink and yellow, heavy rain; green, moderate rain; blue, light rain. (b) Surface analysis corresponding to (a).

breaks of weakly convective rain and drizzle, perhaps with some outbreaks of deeper convection close to the cyclone center. Because of the separate existence of the upper cold front ahead of the surface cold front, this is referred to as a split-front model (Browning and Monk, 1982). Split cold fronts are very common in the United Kingdom. There is much confusion in their analysis when forecasters attempt to apply the simple classical frontal model. To avoid this confusion, the

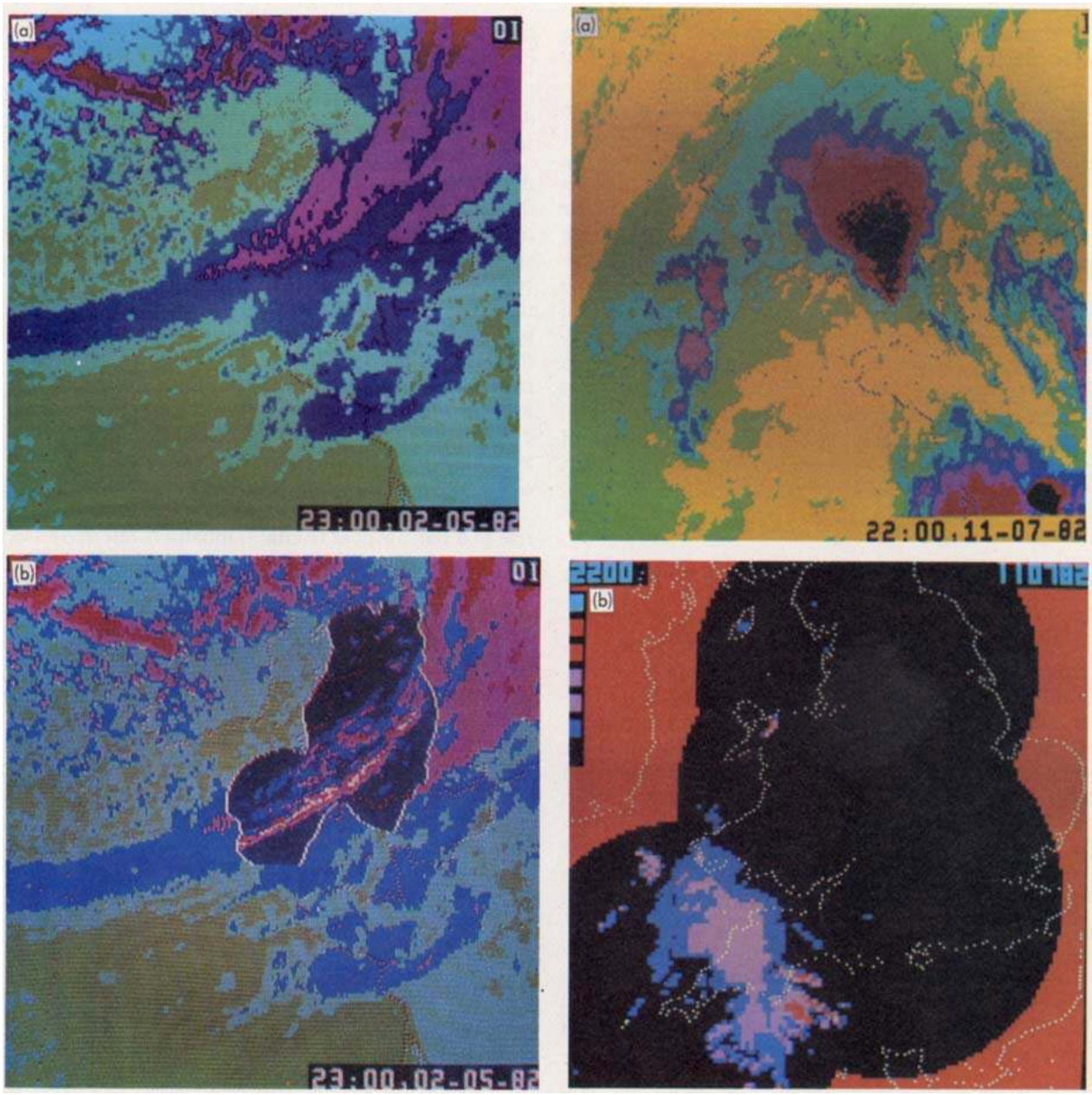

FIG. 9. (a) False-color infrared satellite image from METEOSAT showing a cold frontal cloud band oriented SW–NE across England and Wales. Red and pink, high cloud; dark blue, medium cloud; pale blue, low cloud and cold land; green, sea and warm land. (b) Same as (a) but with data from a network of four radars embedded within it on the same scale and projection. White corresponds to very heavy rain; red, heavy; pink, moderate; blue, light; black, no rain.

FIG. 16. (a) False color infrared satellite image from METEOSAT showing a mesoscale convective system over southwest England. Blue $\leq -52°C$; red $\leq -43°C$; pink $\leq -35°C$; dark blue $\leq -27°C$; pale blue $\leq -16°C$; green $\leq -5°C$; yellow $> -5°C$. The coastlines of the British Isles and France are shown by blue dots. The area of coverage is 1280 km × 1280 km; note that this is four times the area of the companion picture in (b). (b) Rainfall echo distribution at time corresponding to the satellite picture as given by the U.K. weather radar network. Red ≥ 16, mauve ≥ 4, blue ≥ 1 mm h^{-1}.

traditional cold frontal symbolism should be reserved for the surface cold front, and the upper cold front should be identified differently, perhaps by a scalloped line as in Fig. 5a. More often than not, the two fronts are better defined in the humidity (and Θ_w) fields than in the temperature field, in which case they are better regarded as "humidity fronts."

d. The cold conveyor belt

The warm conveyor belt has been identified as the dominant cloud- and precipitation-producing flow in midlatitude systems. A secondary cloud-producing flow is the cold conveyor belt (dotted arrow in Fig. 4), which

originates in the anticyclonic low-level flow to the northeast of a cyclone (Carlson, 1980; Ludlam, 1980). Relative to the advancing cyclone, air in the cold conveyor belt travels westward just ahead of the surface warm front beneath the warm conveyor belt. At first this air subsides and is very dry. Precipitation from the warm conveyor belt evaporates upon falling into it. As it travels westward toward the cyclone center, this air begins to ascend, reaching into the middle troposphere near the apex of the warm sector. Air on the cyclonically sheared edge of the cold conveyor belt, near the surface warm front, experiences enhanced ascent due to frictional convergence. If and when the cold conveyor belt emerges beneath the western edge of the warm conveyor belt, it may ascend anticyclonically and merge with the warm conveyor belt, as sketched in Fig. 4. Alternatively, it may descend cyclonically around the cyclone center. The area of cloud associated with the emerging cold conveyor belt constitutes the head of a large-scale comma cloud system.

3. Classification of mesoscale rainbands in midlatitude frontal systems

The main cloud- and precipitation-producing airstreams have been described above in terms of system-relative flows called conveyor belts. To a first approximation, the rain areas are aligned along these flows. Often the flows are parallel to surface fronts and the belts of precipitation take on a similar orientation. At other times, a conveyor belt may be oriented across a surface front. This happens, for example, in association with an upper cold front, where it overruns the surface warm front. In such a case, the belt of precipitation will be oriented parallel to the upper cold front instead of the underlying warm front.

Precipitation is seldom uniform across a conveyor belt. Convective and mesoscale circulations develop which modulate the distribution of precipitation and lead to quite complex patterns even in the absence of terrain-induced effects. The convection leads to a tendency for the precipitation to concentrate in small-scale cells. The mesoscale circulations are of two kinds. One of them leads to groups of convective cells forming in clusters, giving rise to so-called mesoscale precipitation areas tens of kilometers across. The other, discussed more fully below, leads to banded precipitation features. Sometimes the rainbands are rather uniform along their length; more often they consist of aligned mesoscale precipitation areas. Some rainbands are perhaps no more than mesoscale precipitation areas roughly, and perhaps fortuitously, aligned along the axis of a conveyor belt. Other rainbands are clearly the result of more nearly two-dimensional mesoscale circulations. Considerable attention has been paid to the nature of mesoscale rainbands and many categories have been identified. Broadly speaking, however, there are two principal categories: narrow rainbands and wide rainbands. Examples of these two types are shown in Figs. 6 and 7.

a. Narrow rainbands

Narrow rainbands are largely boundary layer phenomena. Although narrow bands of light rain and drizzle, probably generated by helical vortex circulations, can be generated within warm sectors, the most significant narrow bands are those that occur in the cold seasons at the sharp surface cold-frontal discontinuity in the situations of rearward-sloping ascent described earlier. In the region immediately ahead of the front, the boundary layer can be 2 to 3 km deep, capped by a stable layer. The narrow rainbands that occur here are aligned along the length of the surface front and, even though they are seldom more than 3 km deep and the same in width, they frequently produce a burst of very heavy rain and sometimes small hail.

The band of almost vertical convection that gives rise to a narrow cold frontal rainband is referred to as line convection (Browning and Harrold, 1970). The latter occurs immediately in advance of the cold air, the leading edge of which has the properties of a density current (Carbone, 1982). Its passage is associated with a characteristic temperature drop and pressure kick. The boundary layer ahead of the front is neutrally stratified with respect to saturated ascent, and the density current has the effect of generating convection that

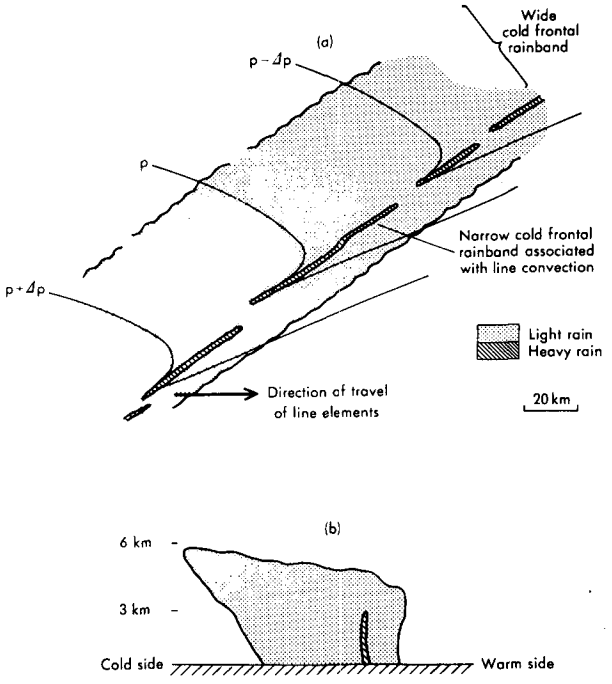

FIG. 8. Schematic depiction of the precipitation distribution at a sharp cold front (a) in plan view and (b) in a vertical section normal to the front.

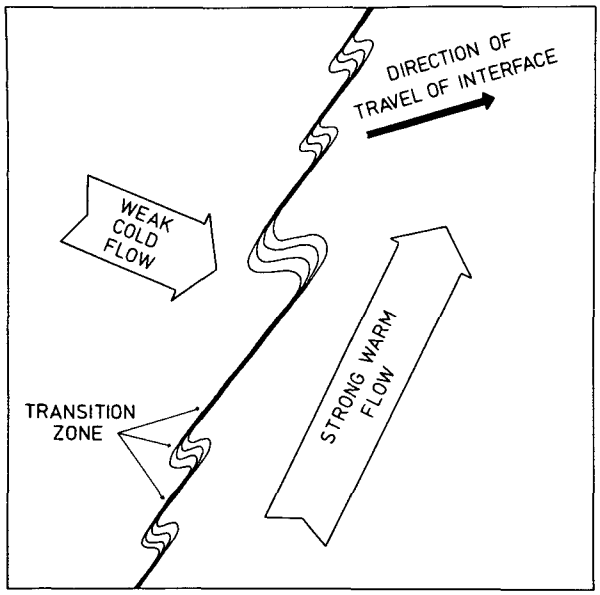

FIG. 10. Schematic depiction of the transition zone at a sharp surface cold front. Line convection elements with intense low-level convergence, strong updrafts and heavy precipitation, occur in the regions with a sharp transition zone. The regions where the temperature gradient is more gradual correspond to gaps between the line convection elements. The broad arrows, representing the flow at low levels on either side of the interface, are drawn relative to the ground (from James and Browning, 1979).

is forced rather than free. Line convection can, on occasion, extend as an unbroken line for 100 km but, more usually, it is broken into series of line elements each of the order of 10 km long. This is associated with a horizontal shearing instability on the strongly sheared edge of the low-level jet that occurs ahead of the front. The resulting rainfall pattern is as shown in Fig. 8 (Hobbs and Biswas, 1979; James and Browning, 1979).

The narrow rainbands associated with the line convection tend to occur toward the leading edge of the belt of stratiform cloud associated with the slantwise convection. Sometimes they occur right at the leading edge, in which case they may be detectable in the satellite imagery. More often, the shallow cumulonimbus associated with the line convection is embedded deep within the main mass of stratiform cloud (Fig. 8); it is then not evident in the satellite imagery (Fig. 9a), although it can be seen clearly by radar (see the white echoes in Fig. 9b).

Narrow rainbands are associated with sharp cold fronts, but such fronts are not uniformly sharp. The sharpest transitions of pressure, wind, temperature and humidity occur at the line elements of the narrow rainband. In the gaps between the elements, there is a more gradual transition, as shown by Fig. 10. When such a gap passes over a surface reporting station, it can give the misleading impression that the surface front is of the diffuse kind normally associated with kata cold fronts.

b. Wide rainbands

The broad zone of generally light-to-moderate rain associated with the slantwise ascent of the conveyor belt often contains organized bands of moderate-to-heavy rain several tens of kilometers wide (Fig. 7a). These are associated with mesoscale circulations within the warm conveyor belt about an axis parallel to the

TABLE 1. Types of wide mesoscale rainbands.

Broad classification	Detailed classification (after Hobbs, 1978)	Frontal archetype with which associated	Location and orientation	Some published examples
Upper (or middle) tropospheric convective rainbands (U-type)	Warm frontal rainband	Forward-sloping ascent	Parallel to the warm front and either on or ahead of it	Browning and Harrold (1969) Herzegh and Hobbs (1978a) Heymsfield (1979)
	Prefrontal cold surge rainband	Forward-sloping ascent	Parallel to and just ahead of an overrunning upper cold front	Kreitzberg (1964) Kreitzberg and Brown (1970) Browning et al. (1973)
	Cold frontal rainband	Rearward-sloping ascent	Parallel to and either behind or straddling an active surface cold front	Browning and Harrold (1969) Hobbs et al. (1978)
Deep convective rainbands	Warm-sector rainband	Either?	Ahead of and parallel to the surface cold front	Nozumi and Arakawa (1968) Herzegh and Hobbs (1978b)
	Postfrontal rainband	Either?	Behind the main frontal system and parallel to the cold front	Houze et al. (1976)

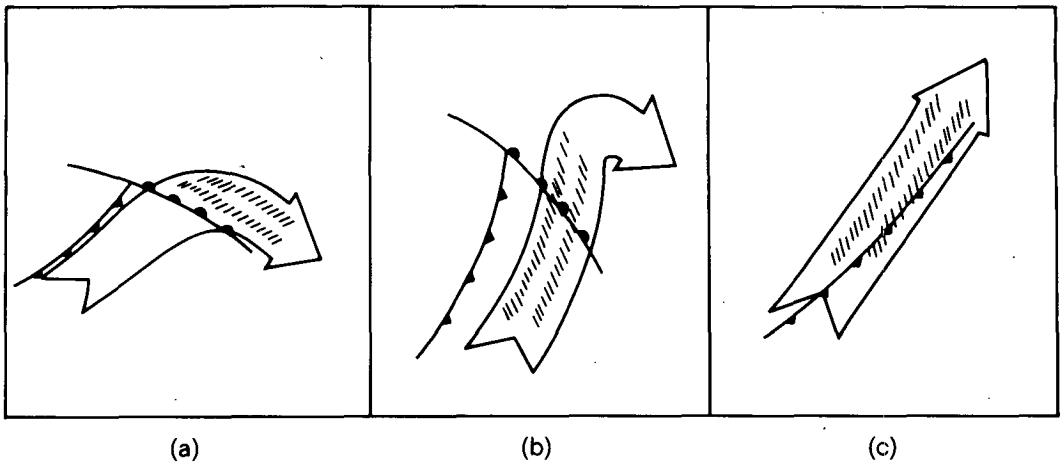

FIG. 11. Idealized representation of three types of configuration of *U*-type wide rainbands (hatched shading) in relation to the warm conveyor-belt flow (broad arrows). (a) and (b) represent forward-sloping ascent situations with warm frontal and prefrontal cold surge rainbands, respectively; (c) represents rearward-sloping ascent with cold frontal rainbands. Narrow rainband elements occur in the boundary layer along the surface cold front coexisting with the wide rainbands in (c).

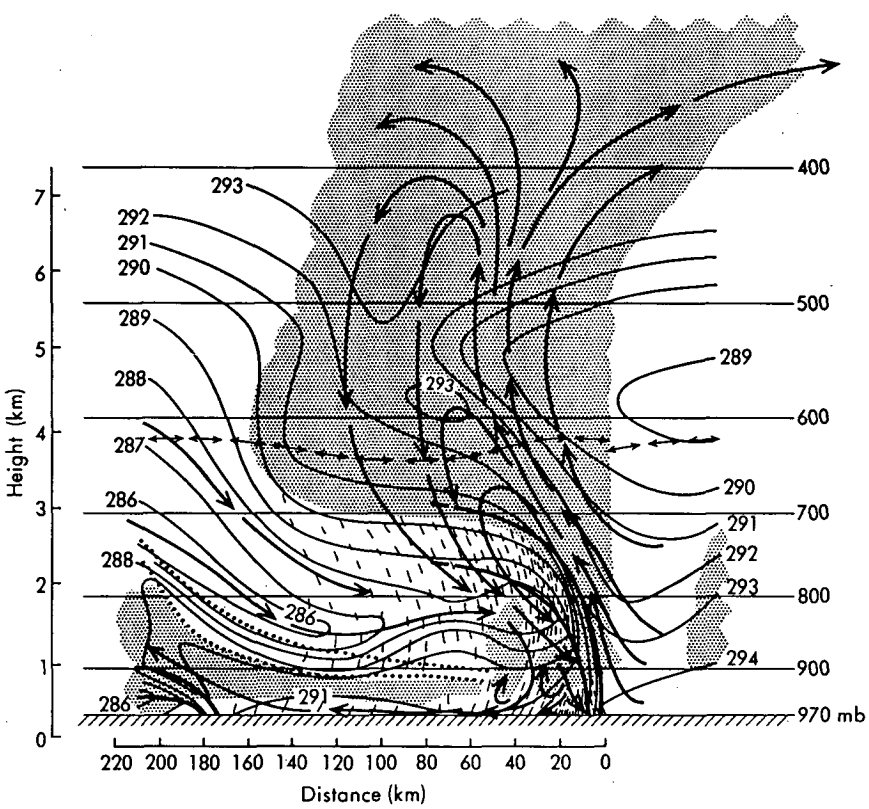

FIG. 12. Vertical section through a squall line (from Newton and Newton, 1959). Heavy lines are boundaries of stable layers, the cold front being far to the left of the squall-line system. Dots indicate a stable layer in the squall sector with shallow clouds beneath and relatively dry sinking air above. Thin lines are isopleths of wet-bulb potential temperature (K). Double-headed arrows represent the melting level. Stippled shading represents cloud. "Raindrops" below cloud base suggest precipitation intensities. Arrows showing overall circulation are schematic.

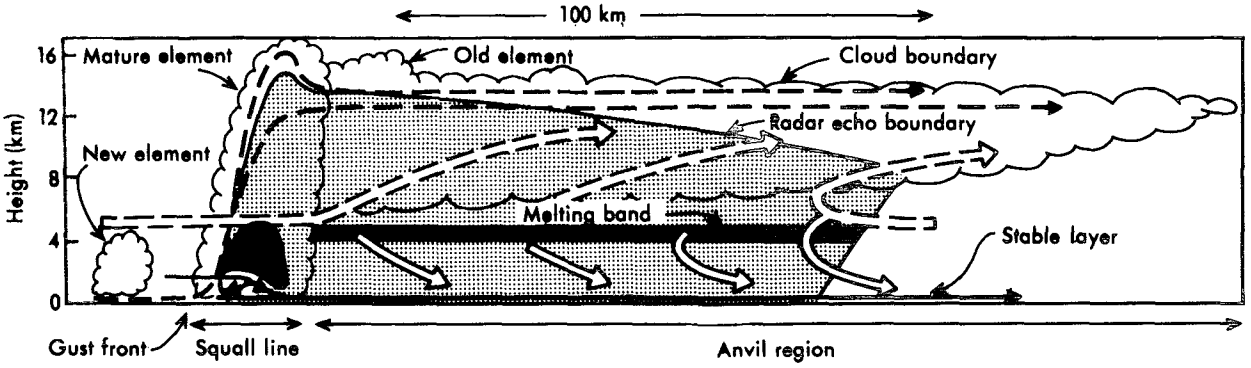

FIG. 13. Schematic depiction of a typical cross section through a tropical squall system. Dashed and continuous streamlines, respectively, show convective-scale updrafts and downdrafts associated with the mature squall-line elements, and also their inflows and outflows. Wide dashed and solid arrows, respectively, show mesoscale updraft and downdraft circulations. Dark shading shows strong radar echo in the melting layer and the heavy precipitation zone of the mature squall-line element. Light shading shows weaker radar echoes. The scalloped line indicates the visible cloud boundary (from Houze and Hobbs, 1982).

relative mean flow. There are several theories to account for them, but one of the most promising is that they are associated with conditional symmetric instability (Bennetts and Hoskins, 1979).

The types of wide rainbands are listed in Table 1. The deep convective rainbands listed are of two kinds. Those occurring in the warm sector are sometimes associated with squall lines (see below). The postfrontal rainbands correspond to the cold-air comma clouds, which are also discussed later. However, the most common type of wide rainband within major frontal systems in the United Kingdom is the upper-level (*U*-type) rainband. Although *U*-type bands may occupy different positions within a frontal system (Fig. 11), they nevertheless all have rather similar dynamical characteristics and can conveniently be considered as one dynamical type. The characteristics of *U*-type rainbands may be summarized as follows:

(i) They are associated with the ascending parts of the warm conveyor belt where its top reaches into the middle troposphere.

(ii) They contain upper- or middle-level convective cells, often in clusters, which are generated within a shallow layer of potential instability where low-Θ_w air overruns the warm conveyor belt. The underlying air is generally statically stable, occasionally markedly so at some levels.

(iii) They are 50-km wide (± a factor of 2) and typically a few hundred kilometers long, with an orientation parallel to the baroclinicity at their level. (The baroclinicity in the lower troposphere is often much stronger and may be oriented differently.)

The structure and evolution of *U*-type rainbands has been described by Kreitzberg and Brown (1970). They use the term "leafed hyper-baroclinic structures" to describe the wrinkling of the surfaces of constant Θ_w in the warm conveyor belt above a frontal zone caused by the mesoscale circulations. Each major wrinkle, or warm tongue, in the conveyor belt gives rise to a separate *U*-type rainband. The wrinkles locally enhance the potential instability and promote the upper- or midtropospheric convective generating cells.

4. Mesoscale convective systems

a. Midlatitude squall lines

The shallow cold frontal line convection discussed above is characterized by a sudden wind shift. However, although the low-level winds ahead of such cold fronts are invariably strong, the sharp veer that occurs at the passage of the line convection is, more often than not, accompanied by a drop in wind speed. The most vigorous squalls, therefore, do not occur in situations of line convection; nor, in general, do they occur in the

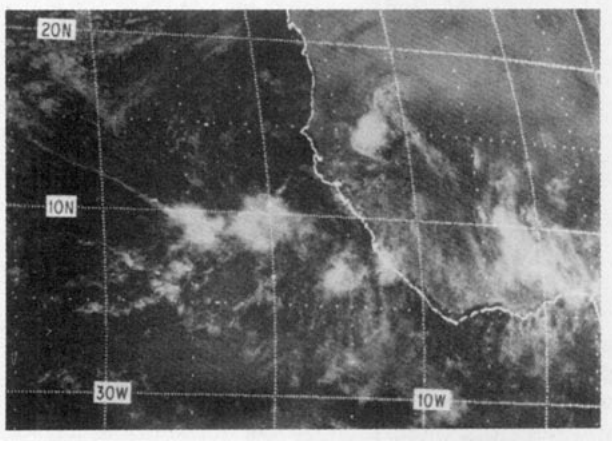

FIG. 14. Visible photograph from the SMS-1 geostationary satellite at 1130 GMT on 5 September 1974 showing tropical cloud systems ranging from fields of small cumulus to large cloud clusters. Cloud clusters are evident from their large cirrus shields at 9°N 24°W, 9°N 21°W, 7°N 16°W, 8°N 12°W, and 14°N 13°W. The last of these was a squall cluster with an arc cloud line on its leading (southwest) side (from Houze and Hobbs, 1982).

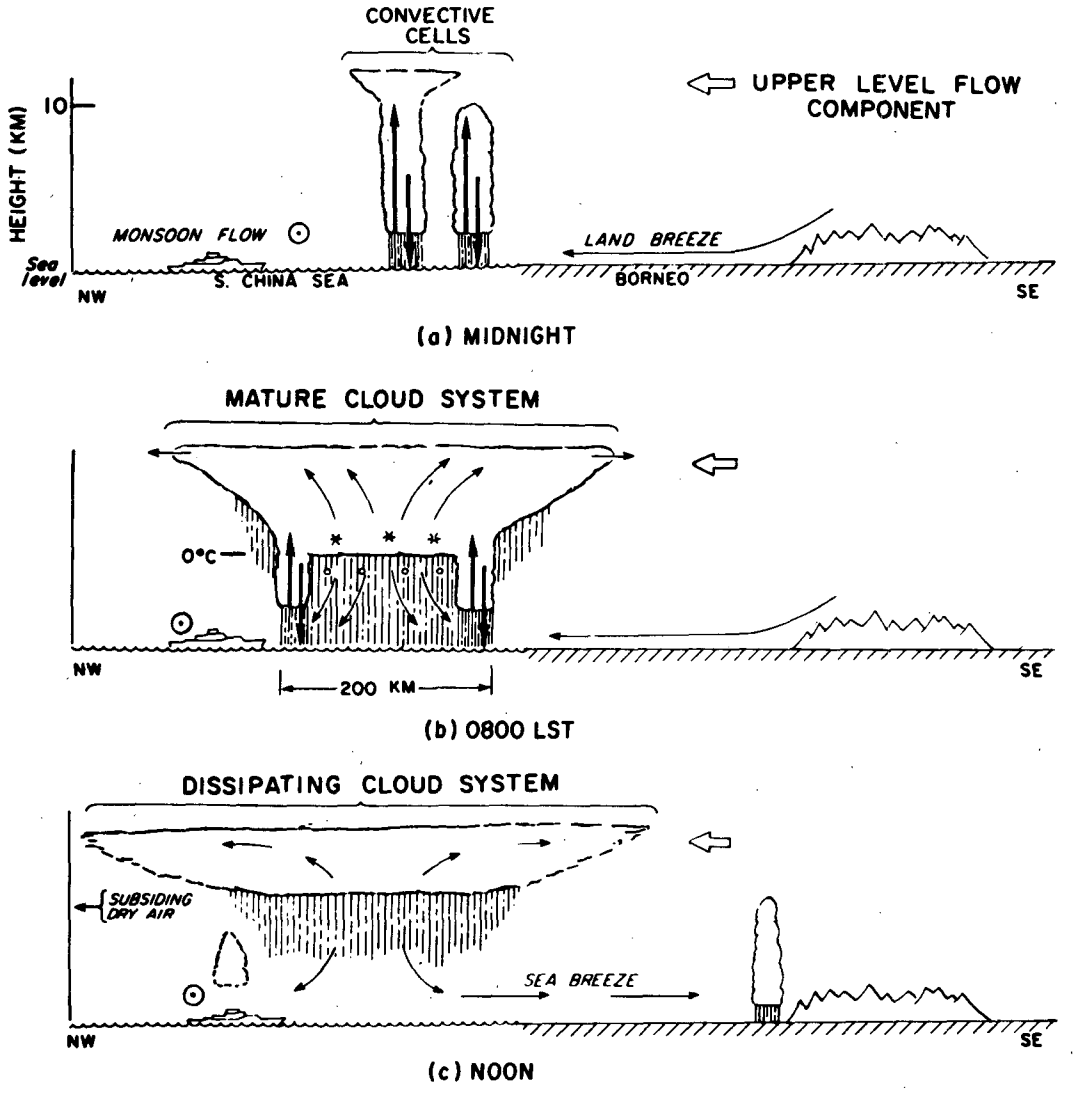

FIG. 15. Schematic depiction of the development of a diurnally generated nonsquall tropical cloud cluster off the coast of Borneo. Various arrows indicate airflow. The circumscribed dot indicates northeasterly monsoon flow out of the page. The wide open arrow indicates the component of the typical east–southeasterly upper-level flow in the plane of the cross section. Heavy vertical arrows in (a) and (b) indicate cumulus-scale updrafts and downdrafts. Thin arrows in (b) and (c) show a mesoscale updraft developing in a mid- to upper-level stratiform cloud with a mesoscale downdraft in the rain below the middle-level base of the stratiform cloud. Asterisks and small circles indicate ice above the 0°C level melting to form raindrops below this level (from Houze et al., 1981).

situations that promote line convection, i.e., where the warm conveyor-belt air undergoes rearward-sloping ascent behind the surface cold front. Instead, major squall lines in middle latitudes occur in association with lines of deep convective cells that break out within warm sectors, often 200–300 km ahead of the surface cold front, in the kind of synoptic situation described in section 2c. This is the situation in which, relative to the large-scale frontal system, the warm conveyor-belt air undergoes forward-sloping ascent ahead of the surface cold front and is overrun by dry, recently descended, air with low Θ_w in the middle troposphere. In the United Kingdom, this synoptic situation usually gives rise to an upper cold front characterized by mid-level convection as in the split-front model in Fig. 5. However, when the value of Θ_w near the ground is high, as often happens in the United States Midwest in the spring storm season, deep convection may occur from the surface. This can lead to vigorous convective cells with strong squalls at the surface forming along or just behind the line corresponding to *UU* in Fig. 5a.

A cross section through a squall line system, (from Newton and Newton, 1959) is shown in Fig. 12. The system, traveling from left to right in the figure, has an

TABLE 2. Criteria used to identify midlatitude mesoscale convective complexes in infrared satellite data (from Maddox, 1980).

	Physical characteristics
Size	A. Cloud shield with continuously low infrared temperatures $\leq -32°C$ must have an area $\geq 100\,000$ km^2 B. Interior cold cloud region with temperature $\leq -52°C$ must have an area $\geq 50\,000$ km^2
Initiation	Size definitions A and B are first satisfied
Duration	Size definitions A and B must be met for a period ≥ 6 h
Maximum extent	Contiguous cold-cloud shield (infrared temperature $\leq -32°C$) reaches maximum size
Shape	Eccentricity (minor axis/major axis) ≥ 0.7 at time of maximum extent
Termination	Size definitions A and B no longer satisfied

organized circulation in the direct solenoidal sense. The moist air of high Θ_w at low levels ahead of the storm ascends steeply through the conditionally unstable air mass. In the case shown here in which the squall line was propagating faster than the cold frontal system, much of the updraft air tends to be left behind the storm as a trailing anvil. In other systems, the anvil may advance mainly ahead of the storm. In either event, the flow in the anvil usually also has a strong component into the plane of Fig. 12. Precipitation falling from the updraft evaporates into dry air that enters the storm circulation at middle levels. Evaporative chilling causes this air to sink by virtue of its increased density. The cold squall-sector air formed in this manner spreads out within an elongated mesohigh pressure region beneath the line of storms. In so doing, the leading edge of the cold air forms a density current or pseudo cold front, which triggers renewed convection there and controls the rate of propagation of the squall line as a whole.

Midlatitude squall lines tend to be segmented into clusters of thunderstorms with overall dimensions of 30–100 km (Fankhauser, 1964; Pedgley, 1962). Just as individual thunderstorms often consist of a number of updraft cells with new ones forming on the right-hand side and old ones dissipating on the left, so too in squall lines the clusters form at the right (southern) end and, after a lifetime of about 5 h, dissipate at the left end.

b. *Tropical squall lines*

Tropical squall lines have an organization similar in many ways to that of midlatitude squall lines except that, being embedded in an easterly flow, they travel toward the west rather than the east, as shown in the conceptual model in Fig. 13. In both cases, the squall lines tend to travel by a combination of cell translation and discrete propagation. New updraft cells in the tropical systems form systematically on the leading edge (left side of Fig. 13), triggered by a density current outflow (gust front) at the surface, which in the tropical squall lines travels westward faster than the winds at any level. These cells grow to become the main cells of the squall line before eventually decaying at the rear. Air having a low Θ_w, originating from middle levels at the front of the storm, feeds negatively buoyant downdrafts within these cells. On reaching the surface, some of the downdraft air spreads forward to produce the gust front, but most of it is left behind as an extensive wake of cool, stable air in the boundary layer. The trailing anvil region aloft has a predominantly stratiform nature. The continued generation of light precipitation aloft in this region implies a zone of mesoscale ascent in the upper troposphere. There is a corresponding zone of mesoscale descent in the lower troposphere.

c. *Tropical nonsquall convective systems*

The visible satellite photograph in Fig. 14 shows tropical cloud systems ranging from fields of scattered small cumulus to mesoscale cloud clusters. One of the clusters produced a squall line, which can be seen as a cloud arc on the southwestern boundary of the cluster. All the other clusters lacked squall line characteristics. Nonsquall cloud clusters are by far the most common form of mesoscale system in the tropics.

The model of a nonsquall cloud cluster in Fig. 15 shows three of the four stages of the life cycle identified by Leary and Houze (1979). The four stages are

1) *Formative stage:* Scattered convective cells are triggered by some initial mesoscale convergence at low levels (Fig. 15a).

2) *Intensifying stage:* Further convective cells form, while existing cells grow and merge, leading to a large continuous area in which the convective cells are interconnected by stratiform precipitation of moderate intensity falling from a spreading anvil deck.

3) *Mature stage:* A mixture of convective and stratiform precipitation exists, as before, but with the area of stratiform precipitation becoming extensive and containing mesoscale updrafts and downdrafts (Fig. 15b).

4) *Dissipating stage:* Rate of formation of new convective cells diminishes, but the area of stratiform upper cloud persists for some time with light rain or virga (Fig. 15c).

Altogether the four stages last about a day, the convective circulations dominating in the early stages and the mesoscale circulations dominating in the later stages.

d. *Mesoscale convective systems in midlatitudes*

Systems resembling tropical cloud clusters also occur in midlatitudes, where they are referred to as mesoscale convective complexes (Zipser, 1982) or systems. The

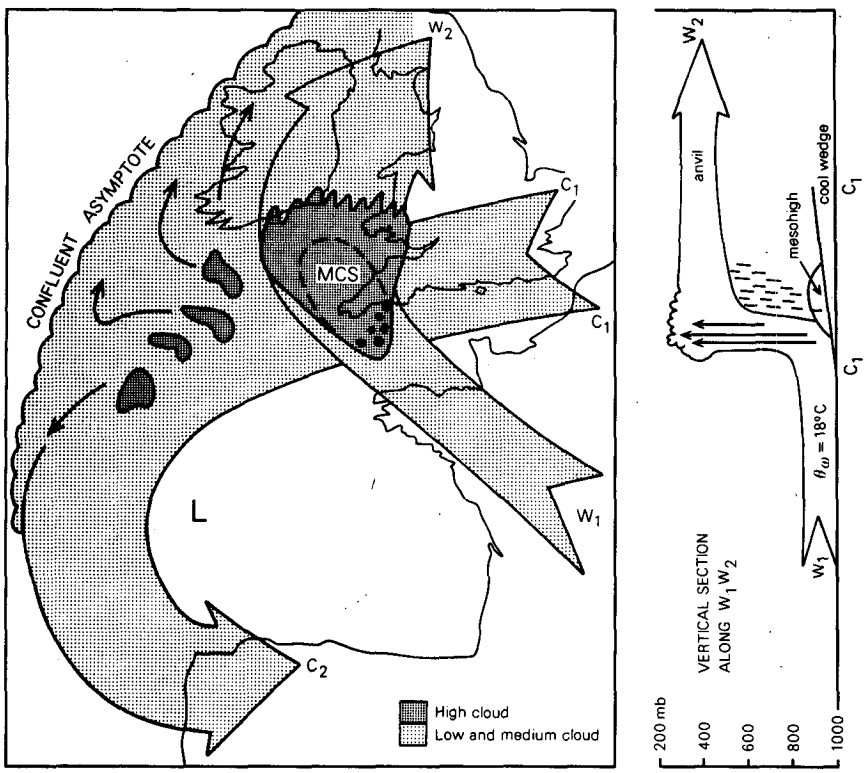

FIG. 17. Schematic model of the mature mesoscale convective system portrayed in Fig. 16 (from Browning and Hill, 1984). Left: plan view. Right: vertical section.

Key to plan view	
Heavy stippled shading	High cirrus shield
Dashed line within MCS	Boundary of surface rain and mesohigh
Blobs in southeast corner of MCS	Convective cores
Arrow W_1W_2	Air with high Θ_w entering MCS below 800 mb and leaving in upper troposphere
Arrow C_1C_2	Cool air circulating around cold pool
Small arrows	Diffluent flow of midtropospheric cloudy air approaching the confluent asymptote
Key to vertical section	
Arrow W_1W_2	Same as arrow in plan section
Vertical arrows	Representation of convective cores
Dashed shading	Mesoscale downdraft
Dome shape	Rain-chilled mesohigh dome
Wedge shape	Wedge of cool surface easterlies associated with arrow C_1C_2

above life-cycle model of Leary and Houze applies to them as well. Their distinctive visual feature is the rather symmetrical upper-level cloud shield generated by the combined anvil outflows from the constituent thunderstorm cells. The top of the cloud shield is high, cold and sharp edged, and it shows up prominently in satellite imagery (Fig. 16a on p. 29). Table 2 shows the criteria used by Maddox to identify mesoscale convective complexes in infrared satellite pictures. The table gives an indication of the large area of many of these systems. However, the particular criteria are unduly restrictive, since there are many smaller systems that appear to have structures and mechanisms similar to those ascribed to mesoscale convective complexes (Zipser, 1982).

Figure 16b shows the precipitation distribution that was associated with the distinctive cloud pattern in Fig. 16a. A mesoscale region of fairly uniform, essentially

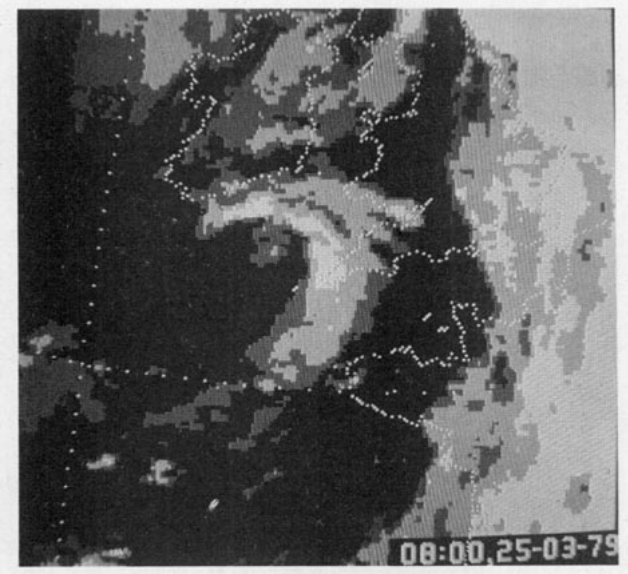

FIG. 18. Level-sliced infrared satellite image from METEOSAT showing a small cold-air comma cloud over southwest England at 0800 GMT on 25 March 1979. Pale grey, high cloud; medium grey, medium cloud; dark grey, low cloud.

stratiform, rain is seen to have developed beneath the cirrus shield downwind (to the northwest) of the active convection. In such situations, thunder may be widespread throughout the areas of both convective and stratiform rain and the whole area may be characterized by a mesohigh produced by evaporative cooling.

Although mesoscale convective systems are dominated by subsynoptic-scale circulations, their development is nevertheless influenced by synoptic-scale forcing. The system portrayed in Fig. 16 formed in a locally intensified baroclinic zone on the flank of a cold pool, and it was fed by a flow of high-Θ_w air (W_1W_2 in Fig. 17), which originated at low levels just ahead of a surface cold front. The configuration of this flow resembles that of the warm conveyor belt in Fig. 4, except that instead of ascending gradually as in most frontal systems, the slantwise ascent is seen to have been short-circuited within the convective updrafts of the mesoscale convective system. This happened where the high-Θ_w flow encountered, and began to ride over, a wedge of cold air (C_1C_2) corresponding to the cold conveyor belt of the model in Fig. 4.

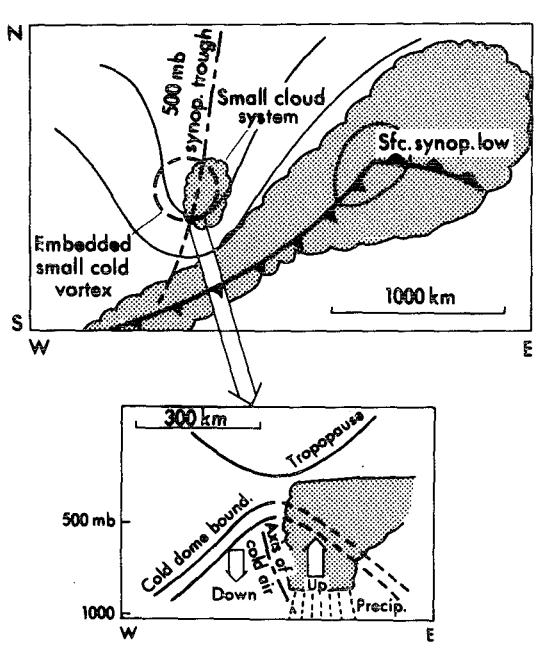

FIG. 19. Schematic representation of a subsynoptic-scale cold vortex (from Matsumoto et al., 1982).

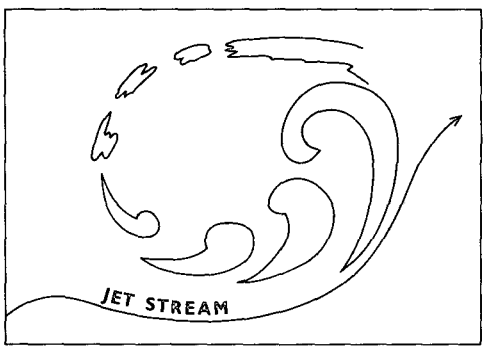

FIG. 20. Schematic representation of successive stages in the life cycle of a subsynoptic-scale comma cloud as it travels around a cold pool behind an upper-level jet stream (from Zick, 1983).

5. Other midlatitude systems

a. Subsynoptic-scale comma clouds associated with cold air vortices

The distinction between frontal, i.e., baroclinic, and convective phenomena tends to be blurred in reality. Thus we have shown that frontal rainbands usually take on a convective character. Likewise, some phenomena often classified as essentially convective can take on frontal characteristics. Nowhere is this dual character more evident than with the comma-shaped cloud and precipitation systems associated with cold pools within polar air streams. Such systems are generally of subsynoptic scale, being spaced at intervals of the order of 1000 km when they occur in multiple form. They develop most often over the oceans in winter, originating in regions of low-level heating and enhanced convection and acquiring the comma-shaped cloud pattern as they mature.

Subsynoptic-scale comma cloud systems occur in association with baroclinicity throughout some or all of the depth of the troposphere and, at the same time, conditional instability through a substantial depth. A wide spectrum of situations can occur, but in all of them the two forms of instability coexist. At one end

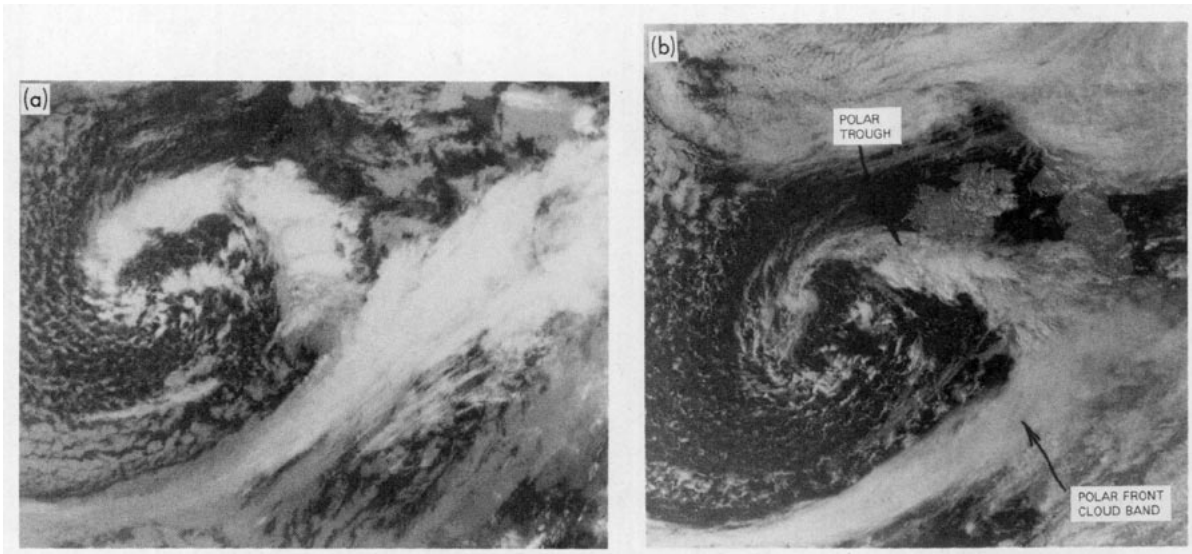

FIG. 21. (a) Infrared photograph from an NOAA satellite at 0817 GMT and (b) visible photograph from another satellite pass at 1502 GMT on 9 September 1983. (a) shows a convective cloud band (associated with a polar-trough conveyor belt) wrapped around the leading edge of a cold pool and situated in close proximity to a stratiform cloud band (associated with a polar-front conveyor belt). A few hours later, as shown in (b), the two cloud bands merged to form a lambda-shaped pattern (Courtesy University of Dundee).

of the spectrum are the polar lows that form in very cold northerly outbreaks over warm oceans (e.g., off the Norwegian coast) in which convection is vigorous and a CISK mechanism appears to be the more important driving force (Rasmussen, 1983). At the other end of the spectrum are those comma clouds in which baroclinic slantwise ascent is the primary driving force. This seems to be the case for the short-wave polar troughs commonly encountered in the westerly flows behind major cold fronts approaching the northwest of Europe and the United States (Reed, 1979; Locatelli et al., 1982). An example of a comma cloud associated with a polar trough is shown in Fig. 18. The axis of the trough is situated along the trailing edge of the comma cloud. The subsynoptic-scale flow responsible for the comma cloud is like a diminutive version of the warm conveyor belt discussed in section 2a. The comma cloud zone is characterized by convective precipitation, and also by a distinct low-level jet, as in the case of the synoptic-scale warm conveyor belt ahead of a cold front. Fox (1982) has shown that this is true even for very small polar air systems.

Subsynoptic-scale comma cloud systems usually develop near the leading edge of a cold pool behind a

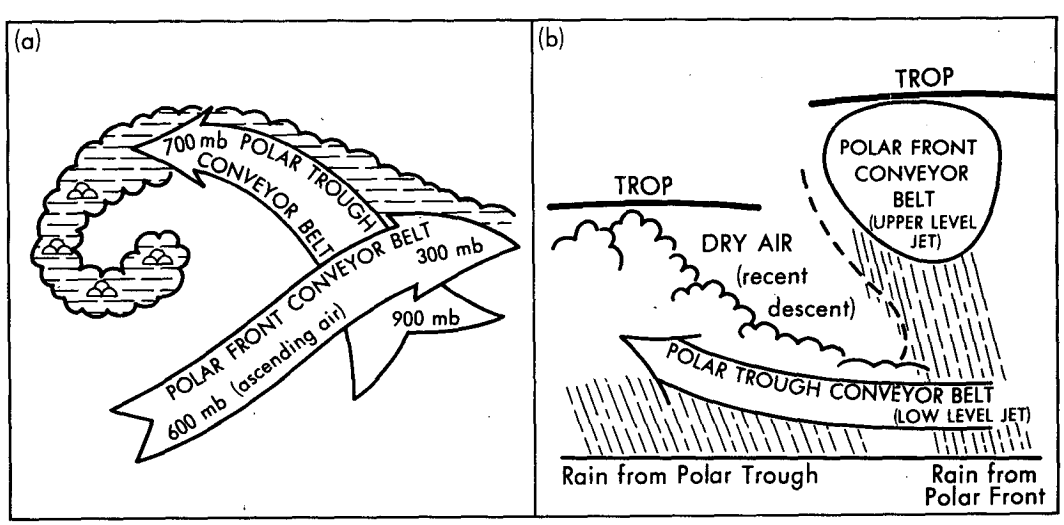

FIG. 22. Schematic model of the cloud system in Fig. 21, showing intersecting polar-trough conveyor belt and polar-front conveyor belt: (a) plan view and (b) vertical section along axis of polar trough (from Browning and Hill, 1985).

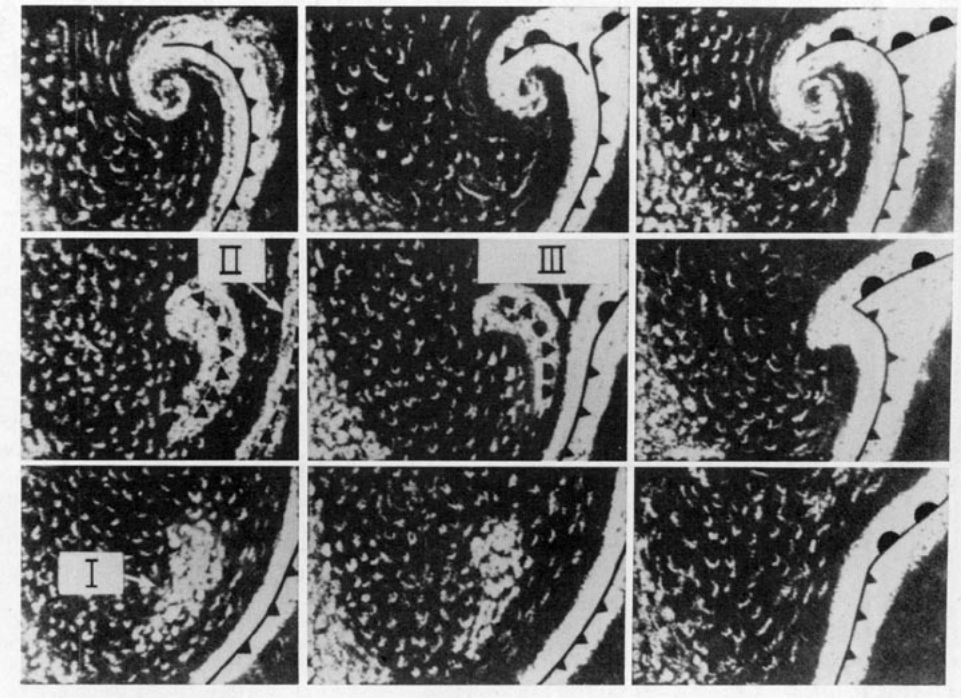

FIG. 23. Schematic depiction of three basic sequences of vortex development evident in satellite imagery: (a) development of a comma cloud entirely within the cold air, (b) development of an instant occlusion, (c) development of a frontal wave. The figure (adapted from Zillman and Price, 1972) was derived from observations over the Southern Ocean, but it is printed vertically inverted so as to apply to the Northern Hemisphere. Frontal symbols indicate one scheme for representing the various evolution sequences using the tools of conventional frontal analysis. The labels I, II and III indicate a region of enhanced convection, a decaying cloud band and a convective cloud band merging with the frontal cloud band, respectively.

major frontal system (Fig. 19). According to Matsumoto et al. (1982), the cloud penetrates through the upper boundary of the cold dome and reaches the level of the tropopause, which is low in such regions. When cloud from the preceding frontal system gets carried around the back of the cold pool, to give what synopticians refer to as a back-bent occlusion, comma clouds may develop from elements of this cloud as they travel around the southern flank of the cold pool (Fig. 20).

b. The polar-trough conveyor belt and instant occlusion

An instant occlusion is the name given to the lambda-shaped cloud pattern produced when a cloud band associated with a polar trough interacts with a cloud band associated with the polar front (Reed, 1979; Zillman and Price, 1972; Thepenier and Cruette, 1981; Weldon, 1975). Figure 21 shows an example of a variant of the instant occlusion referred to as a pseudo-occlusion. Figure 21a shows an early stage in its development, just before the two cloud bands merge to produce the characteristic lambda pattern shown in Fig. 21b. This process is interpreted by Browning and Hill (1985) in terms of a dual conveyor-belt configuration, with two small conveyor-belt flows intersecting at right angles, as shown in Fig. 22. The feature labeled polar-front conveyor belt corresponds to a warm conveyor belt ascending as an upper-tropospheric jet streak. The polar-trough conveyor belt corresponds to a low-level jet with an associated cloud band extending above it on the poleward side of the polar front. This low-level jet is situated beneath the left exit of the upper jet streak and may be part of an ageostrophic circulation forced by the latter (Uccellini and Johnson, 1979). Although having a disposition similar to the cold conveyor belt in Fig. 4, the polar-trough conveyor belt is, in fact, characterized by a local maximum in Θ_w, the air being drawn polewards at low altitudes, as it were, from the tip of an ill-defined warm sector. Far from being associated with a classical occlusion process, the air within the polar-trough conveyor belt has its greatest positive anomaly of temperature and humidity in the lowest kilometer or two. Cooler, drier air circulating around the low center overruns the polar-trough con-

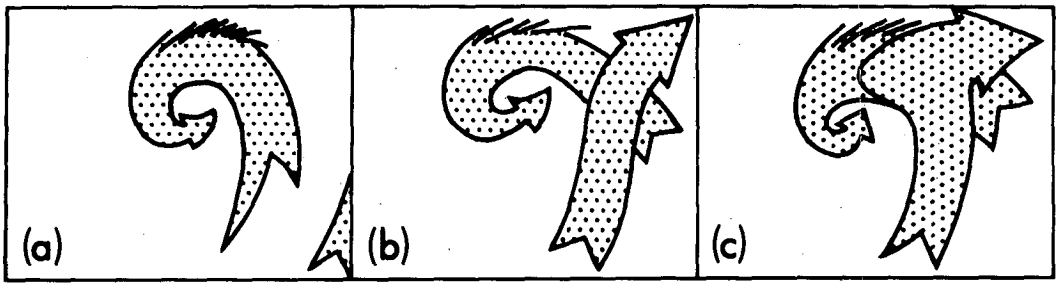

FIG. 24. Schematic depiction of the conveyor-belt flows associated with the cloud patterns at time t_3 in Figs. 23a, b and c.

veyor belt leading to outbreaks of convective precipitation within it.

The instant or pseudo-occlusion can be thought of as part of a spectrum of types (Figs. 23 and 24) in which the form of the disturbance depends on the position of the short-wave trough or vorticity maximum with respect to the polar front (Zillman and Price, 1972). The simple comma-cloud development represented in Fig. 23a shows the short-wave trough and associated vorticity maximum occurring well within the cold air and not interacting significantly with the main polar front (Fig. 24a). By contrast, when the vorticity maximum is at the latitude of the polar front (Fig. 23c), a frontal wave forms in which the main warm conveyor belt associated with the polar front gets involved in the circulation and dominates the cloud pattern (Fig. 24c). In the intermediate situation of the instant or pseudo-occlusion (Figs. 23b and 24b), there are two distinct cloud belts, associated with the polar trough and the polar front.

REFERENCES

Bennetts, D. A., and B. J. Hoskins, 1979: Conditional symmetric instability—a possible explanation for frontal rainbands. *Quart. J. Roy. Meteor. Soc.*, **105,** 945–962.

Browning, K. A., and T. W. Harrold, 1969: Air motion and precipitation growth in a wave depression. *Quart. J. Roy. Meteor. Soc.*, **95,** 288–309.

——, and ——, 1970: Air motion and precipitation growth at a cold front. *Quart. J. Roy. Meteor. Soc.*, **96,** 369–389.

——, and C. W. Pardoe, 1973: Structure of low-level jet streams ahead of mid-latitude cold fronts. *Quart. J. Roy. Meteor. Soc.*, **99,** 619–638.

——, and G. A. Monk, 1982: A simple model for the synoptic analysis of cold fronts. *Quart. J. Roy. Meteor. Soc.*, **108,** 435–452.

——, and F. F. Hill, 1984: Structure and evolution of a mesoscale convective system near the British Isles. *Quart. J. Roy. Meteor. Soc.*, **110,** 897–913.

——, and ——, 1985: Mesoscale analysis of a polar trough interacting with a polar front. *Quart. J. Roy. Meteor. Soc.*, **111,** 445–462.

——, M. E. Hardman, T. W. Harrold and C. W. Pardoe, 1973: The structure of rainbands within a mid-latitude depression. *Quart. J. Roy. Meteor. Soc.*, **99,** 215–231.

Cahir, J. J., G. S. Forbes, W. D. Lottes and T. Staskiewicz, 1986: Structural aspects of the warm conveyor. (Submitted for publication).

Carbone, R. E., 1982: A severe frontal rainband. Part I: Stormwide hydrodynamic structure. *J. Atmos. Sci.*, **39,** 258–279.

Carlson, T. N., 1980: Airflow through midlatitude cyclones and the comma cloud pattern. *Mon. Wea. Rev.*, **108,** 1498–1509.

Fankhauser, J. C., 1964: On the motion and predictability of convective systems. Rep. No. 21, National Severe Storms Projects.

Fox, A. D., 1982: Vertical structure and dynamics of mesoscale wave disturbance inferred from GOES satellite imagery and ground truth data. *Proc. Ninth Conf. on Weather Forecasting and Analysis,* Seattle, Amer. Meteor. Soc., 152–159.

Green, J. S. A., F. H. Ludlam and J. F. R. McIlveen, 1966: Isentropic relative-flow analysis and the parcel theory. *Quart. J. Roy. Meteor. Soc.*, **92,** 210–219.

Harrold, T. W., 1973: Mechanisms influencing the distribution of precipitation within baroclinic disturbances. *Quart. J. Roy. Meteor. Soc.*, **99,** 232–251.

Herzegh, P. H., and P. V. Hobbs, 1978a: Air motions and precipitation growth in a mesoscale precipitation band associated with a warm front. *Proc. 18th Conf. on Radar Meteorology,* Atlanta, Amer. Meteor. Soc., 23–28.

——, and ——, 1978b: Generating cells and precipitation growth in mesoscale rainbands. *Proc. Conf. on Cloud Physics and Atmospheric Electricity,* Issaquah, WA, Amer. Meteor. Soc., 284–291.

Heymsfield, G. M., 1979: Doppler radar study of a warm frontal region. *J. Atmos. Sci.*, **36,** 2093–2107.

Hobbs, P. V., 1978: Organization and structure of clouds and precipitation on the mesoscale and microscale in cyclonic storms. *Rev. Geophys. Space Phys.*, **16,** 741–755.

——, and K. R. Biswas, 1979: The cellular structure of narrow cold-frontal rainbands. *Quart. J. Roy. Meteor. Soc.*, **105,** 723–727.

——, J. D. Locatelli, J. T. Matejka and R. A. Houze, Jr., 1978: Air motions, mesoscale structure and cloud microphysics associated with a cold front. *Proc. Conf. on Cloud Physics and Atmospheric Electricity,* Issaquah, WA, Amer. Meteor. Soc., 277–283.

Houze, R. A., Jr., and P. V. Hobbs, 1982: Organisation and structure of precipitating cloud systems. *Adv. Geophys.*, **24,** 225–315.

——, ——, K. R. Biswas and W. M. Davis, 1976: Mesoscale rainbands in extratropical cyclones. *Mon. Wea. Rev.*, **104,** 868–878.

——, S. G. Geotis, F. D. Marks, Jr. and A. K. West, 1981: Winter monsoon convection in the vicinity of North Borneo. Part I: Structure and time variation of the clouds and precipitation. *Mon. Wea. Rev.*, **109,** 1595–1614.

Hsie, E. Y., R. A. Anthes and D. Keyser, 1984: Numerical simulation of frontogenesis in a moist atmosphere. *J. Atmos. Sci.*, **41,** 2581–2594.

James, P. K., and K. A. Browning, 1979: Mesoscale structure of line convection at surface cold fronts. *Quart. J. Roy. Meteor. Soc.*, **105,** 371–382.

Kreitzberg, C. W., 1964: The structure of occlusions as determined from serial ascents and vertically-directed radar. Rep. AFCRL-64-26, Air Force Cambridge Research Laboratories, Bedford, MA, 121 pp.

——, and H. A. Brown, 1970: Mesoscale weather systems within an occlusion. *J. Appl. Meteor.*, **9,** 417–432.

Leary, C. A., and R. A. Houze, Jr., 1979: The structure and evolution

of convection in a tropical cloud cluster. *J. Atmos. Sci.*, **36,** 437–457.

Locatelli, J. D., P. V. Hobbs and J. A. Werth, 1982: Mesoscale structure of vortices in polar air streams. *Mon. Wea. Rev.*, **110,** 1417–1433.

Ludlam, F. H., 1980: *Clouds and Storms.* Pennsylvania State University Press, 405 pp.

Maddox, R. A., 1980: Mesoscale convective complexes. *Bull. Amer. Meteor. Soc.*, **61,** 1374–1387.

Matsumoto, S., K. Ninomiya, R. Hasegawa and Y. Miki, 1982: The structure and the role of a subsynoptic-scale cold vortex on the heavy precipitation. *J. Meteor. Soc. Japan,* **60,** 339–354.

Miles, M. K., 1962: Wind temperature and humidity distribution at some cold fronts over SE England. *Quart. J. Roy. Meteor. Soc.*, **88,** 286–300.

Newton, C. W., and H. R. Newton, 1959: Dynamical interactions between large convective clouds and environment with vertical shear. *J. Meteor.*, **16,** 483–496.

Nozumi, Y., and H. Arakawa, 1968: Prefrontal rainbands located in the warm sector of subtropical cyclones over the ocean. *J. Geophys. Res.*, **73,** 487–492.

Pedgley, D. E., 1962: A meso-synoptic analysis of the thunderstorms on 28 August 1968. *Geophys. Mem.*, 14, No. 106, Meteorological Office, Her Majesty's Stationery Office.

Rasmussen, E., 1983: A review of mesoscale disturbances in cold air masses. *Mesoscale Meteorology—Theories, Observations and Models,* D. K. Lilly and T. Gal-Chen, Eds., Reidel, 247–283.

Reed, R. J., 1979: Cyclogenesis in polar air streams. *Mon. Wea. Rev.*, **107,** 38–52.

Ryan, B. F., and K. J. Wilson, 1985: The Australian summertime cool change. Part III: Subsynoptic and mesoscale model. *Mon. Wea. Rev.*, **113,** 224–240.

Sansom, H. W., 1951: A study of cold fronts over the British Isles. *Quart. J. Roy. Meteor. Soc.*, **77,** 96–120.

Thepenier, R. M., and D. Cruette, 1981: Formation of cloud bands associated with the American subtropical jet stream and their interaction with midlatitude synoptic disturbances reaching Europe. *Mon. Wea. Rev.*, **109,** 2209–2220.

Uccellini, L. W., and D. R. Johnson, 1979: The coupling of upper and lower tropospheric jet streaks and implications for the development of severe convective storms. *Mon. Wea. Rev.*, **107,** 682–703.

Weldon, R. B., 1975: Satellite training course notes. Part II. The structure and evolution of winter storms. Unpublished lecture notes, Applications Division, National Environmental Satellite Services, U.S. Dept. of Commerce, NOAA.

——, 1979: Satellite training course notes. Part IV. Cloud patterns and the upper air wind field. AWS TR-79 003, U.S. Air Force.

Zick, C., 1983: Method and results of an analysis of comma cloud developments by means of vorticity fields from upper tropospheric satellite wind data. *Meteor. Rundsch.*, **36,** 69–84.

Zillman, J. W., and P. G. Price, 1972: On the thermal structure of mature Southern Ocean cyclones. *Aust. Meteor. Mag.*, **20,** 34–48.

Zipser, E. J., 1982: Use of a conceptual model of the life-cycle of mesoscale convective systems to improve very-short-range forecasts. *Nowcasting,* K. A. Browning, Ed., Academic Press, 191–204.